SAR Imagery Applied to the Monitoring of Hyper-Saline Deposits: Death Valley Example (CA)

Yannick Lasne[1], Philippe Paillou[2], Anthony Freeman[1], and Bruce Chapman[1]

***Abstract*—The present study aims at understanding the inf uence of salinity on the dielectric constant of soils and then on the backscattering coeff cients recorded by airborne / spaceborne SAR systems. Based on dielectric measurements performed over hyper-saline deposits in Death Valley (CA), as well as laboratory electromagnetic characterization of salts and water mixtures, we used the dielectric constants as input parameters of analytical IEM simulations to model both the amplitude and phase behaviors of SAR signal at C, and L-bands. Our analytical simulations allow to reproduce specif c copolar signatures recorded in SAR data, corresponding to the Cottonball Basin saltpan. We also propose the copolar backscattering ratio and phase difference as indicators of moistened and salt-affected soils. More precisely, we show that these copolar indicators should allow to monitor the seasonal variations of the dielectric properties of saline deposits.**

***Index Terms*—ALOS/PALSAR, AIRSAR, evaporites, copolar phase difference, Death Valley, IEM, radar backscattering, salinity, SAR, soil moisture, SIR-C.**

I. Introduction

SOIL salinization in arid and semi-arid regions still remains one of the most important threats not only for socio-economical issues when dealing with water ressources management, but also for ecological matters such as: desertif cation, climate changes, and biomass reduction. Then, monitoring and mapping of soil salinity distribution represent today a key challenge in our understanding of such environmental processes.

Being highly dependent on the dielectric properties of soils, synthetic aperture radar (SAR) appears to be an eff cient tool for the remote sensing of hyper-saline environments [1]-[4]. More precisely, the inf uence of saline deposits on SAR imagery lies in the solubility and ionic properties of the minerals which strongly inf uence both real and imaginary parts of the complex permittivity of such deposits, and thus the radar backscattering coeff cient [5]-[7].

Although some studies focused on the establishment of dielectric mixing model taking into account the salinity effect [8]-[10], few attempts have been performed to describe the inf uence of salinity on the radar backscattering coeff cient [5], [11], [12]. Moreover, very little study have been done on the large amount of available SAR data [1]-[4].

Based on temporal series acquired with spaceborne SAR systems (ALOS/PALSAR, SIR-C) over the Death Valley (CA), we show that the copolarized backscattering ratio and phase difference derived from SAR data can be used as suitable indicators to monitor the dynamics of hyper-saline deposits. In particular, we propose these copolar parameters to follow the variations in the dielectric properties of moistened and salt-affected soils on a seasonal time scale because of the close relationship between the salinity (governed by the soil moisture content) and the complex permittivity of the soils. We also highlight a strong temporal correlation between the copolar parameters and weather data since precipitation events control the soil moisture and salinity.

In order to allow for a better interpretation of the saline deposits signatures observed on SAR data, we also perform analytical simulations of the radar backscattering associated with saline deposits by means of the IEM scattering model. Using laboratory and $in\ situ$ dielectric measurements as input parameters, we simulate the copolar ratio and phase difference as function of the complex permittivity and surface roughness. Successfully reproducing the observed signature, our results indicate that the analysis of SAR data could also account for the monitoring and understanding of seasonal changes of evaporitic basins through a close correlation between the soil moisture and surface roughness related to the desiccation processes.

[1]Jet Propulsion Laboratory, California Institute of Technology (NASA), Pasadena, CA, USA (e-mail: ylasne@jpl.nasa.gov).

[2]Observatoire Aquitain des Sciences de l'Univers, LAB-UMR 5804, Floirac, France.

Such results are of great interest for soil salinity monitoring and the detection of small amounts of subsurface water mixed with evaporites, not only for arid terrestrial surfaces but also for planetary missions, particularly the exploration of Mars.

II. Problem of Salinity

In microwave remote sensing, it is now well known that the radar backscattering coefficient of a target is highly sensitive to its electrical properties through the permittivity and the conductivity, that is the complex dielectric constant of the material, [13]-[14]. While the influence of moisture on the backscattering coefficient has been extensively investigated over the last two decades [15]-[19], few attempts have been performed in order to describe the effect of salinity on the radar backscattering [2], [5], [11] - [12], [20]. Moreover, very little study has been performed on the large amount of available SAR data (ERS, JERS, RADARSAT, SIR-C/X-SAR, AIRSAR, and ALOS/PALSAR) [2]-[4], [12], [21] - [22]. Based on laboratory measurements, Shao *et al.* [3] confirmed that the frequency and the salinity of soils have little influence on the real part of the dielectric constant while the imaginary part is strongly affected by both salinity and moisture of soil samples, especially in the [1-6GHz] frequency range. Using RADARSAT-1 images, these authors also highlighted a strong correlation between the backscattering coefficient extracted from SAR data and the imaginary part of the complex permittivity, simultaneously measured on soil samples of the illuminated scene. More recently, based on RADARSAT-1 images acquired over the Wadi El-Natrun site (Egypt), Aly [2] proposed a parametric formulation in order to evaluate the ability of RADARSAT-1 SAR system to monitor the salt content of soils by means of the combination of three SAR modes (S1, S3, and S5), without any use of backscattering models. Using ERS-1 images acquired over the Chott El Djerid (Tunisia), Wadge *et al.* [4] investigated the potential of the ERS-1 SAR system to infer the evaporation rate for this widespread hyper-saline environment. Assuming an empirically derived relationship between radar backscatter and surface roughness, due to evaporation resulting in halite crystal efflorescence, these authors converted the ERS-1 backscatter time series into rates of halite growth. Under the assumption that the temporal change of roughness is proportional to the increase of halite mass derived from evaporation, they estimated the volume of water evaporated during the halite crystal crust layer formation. They shown that the evaporation rates derived from radar data are two to three times those measured on the pan. If they suggested additional surface roughening agent(s) to account for the overestimation of evaporation by their radar method, an alternative explanation would be an underestimation of the dielectric properties of the Chott El Djerid saltpan. Using AIRSAR data acquired over Alligator River Region in Australia, Bell *et al.* inferred estimates of the complex permittivity for soil salinity discrimination based on the analysis of the copolar correlation coefficient. All these studies highlight the importance of salinity in microwave remote sensing.

III. Airborne and Spaceborne SAR Data Analysis

In order to assess the influence of saline deposits on SAR imagery, several sets of SAR images were considered. The first data set was acquired by the SIR-C spaceborne system which provides us with a temporal series for April and October-September 1994 periods at both L- and C-bands. The second one was obtained by means of the airborne AIRSAR sensor on April 10, 1994 at P-, L-, and C-bands. Additionnally, we considered a recent temporal series acquired by the japenese ALOS/PALSAR sensor at L-band, providing 6 sets of SAR images between 2006 and 2008. Figures 1 and 2 display AIRSAR and SIR-C images corresponding to the test site under consideration (saltpan of Cottonball Basin in Death Valley), while Figure 3 displays an example of the copolar parameters extracted from the SIR-C PR11317 data. The saltpan can be clearly observed in all Figures.

Table I summarizes the mean values of the copolarized ratio and phase difference extracted from spaceborne and airborne SAR data corresponding to the test site area (black polygon).

The copolar ratio suggests a seasonal effect related to a change in soil moisture. For SIR-C data, it can be clearly observed that σ_{hh}/σ_{vv} increases

Fig. 1. AIRSAR cm6507 image of Death Valley displaying the total power recorded in the three frequencies: P-band (red), L-band (green), and C-band (blue). (Credit: NASA/JPL).

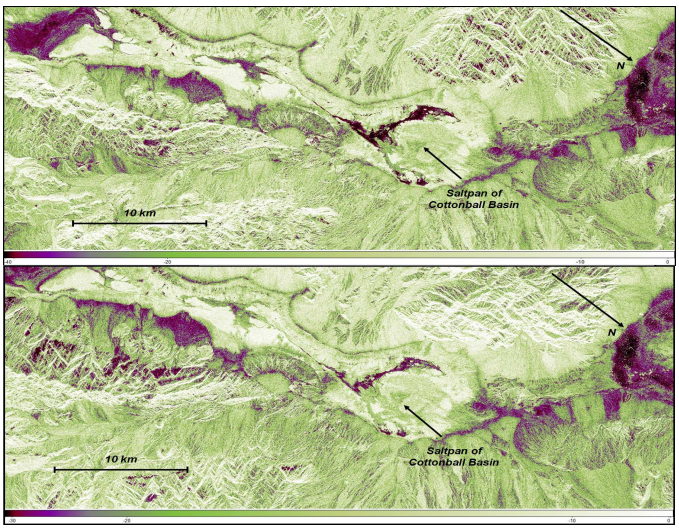

Fig. 2. Temporal series of L-Band SIR-C images for HH polarization [dB]. The acquisition dates are April 16th (PR11317, top) and Spetember 30th (PR50315, bottom), 1994. Cottonball Basin is clearly observed in the center of the images, revealing a specif c signature at the location of saline deposits (arrow).

between April and September for both C and L-bands. According to the yearly distribution of the precipitation, such an increase can be related to the weather and climatic conditions described in [23], [24]. During the wet season (April), the precipitation events lead to high soil moisture content, combined with small roughness parameter: the surface sodium chloride crust is dissolved by fresh water discharges. Such low roughness conditions better separate HH and VV behaviours, we then logically observe the smallest copolarized ratios in April on SAR data. On the contrary, during the dry season (September), the low soil moisture conditions, coupled to the desiccation of the crystal crust layer, lead to an increase in surface roughness. According to [25] and [26], such an increment in the roughness parameters should lead to an increase in the σ_{hh}/σ_{vv}, since for rough surfaces the isotropic scattering distribution

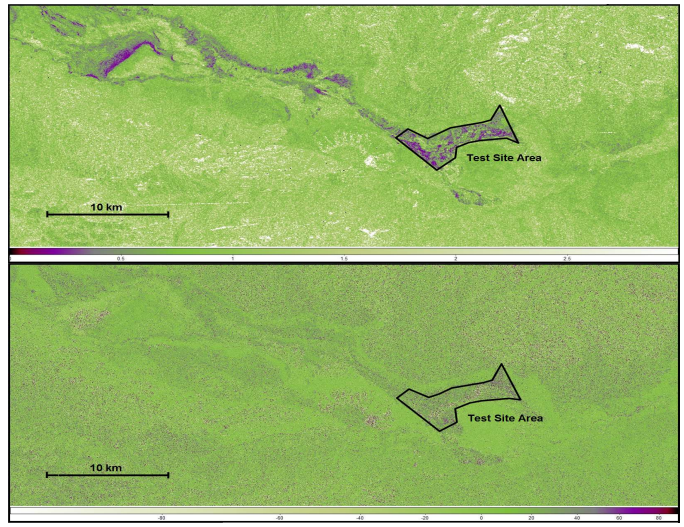

Fig. 3. Copolar backscattering ratio (top) and phase difference (bottom) derived from the SIR-C PR11317 acquisition. Typical σ_{hh}/σ_{vv} and ϕ_{HH-VV} signatures can be clearly observed and related to the presence of saline deposits delimited by the black polygon.

leads to the same HH and VV backscattering coeff cients. As expected, σ_{hh}/σ_{vv} presents an increase in September. The stronger increase observed for C-band compared to L-band can give some information on the roughness parameters, since the roughness effect is stronger at scales on the order of the wavelength. In summary, variations of the copolarized ratio ref ect the seasonal variation of the rainfall through the dependency of σ_{hh}/σ_{vv} on the soil moisture content and surface roughness.

As shown on Fig. 4, such a correlation between the copolar parameters and the weather data also clearly appears on the ALOS/PALSAR temporal series. It can be clearly observed that the increase in σ_{hh}/σ_{vv} corresponds to the dry season (low rainfall associated to high wind speed and high temperatures leading to high evaporation rate). As previously mentioned, the resulting desiccation effect lead to higher surface roughness parameters suitable to increase in σ_{hh}/σ_{vv}. On the contrary, following the wet season, a decrease in σ_{hh}/σ_{vv} can be observed.

Dealing with the copolar phase difference, we showed in previous studies that this phase signal could be used as a moisture indicator [27], [28]. Since the expression of ϕ_{HHVV} is derived from the copolar backscattering coeff cients, the different behavior of the backscattering coeff cients in each copolarized mode, as revealed by σ_{hh}/σ_{vv}, can impact the phase signal. We then proceeded with the same analysis for ϕ_{HHVV} as the one performed

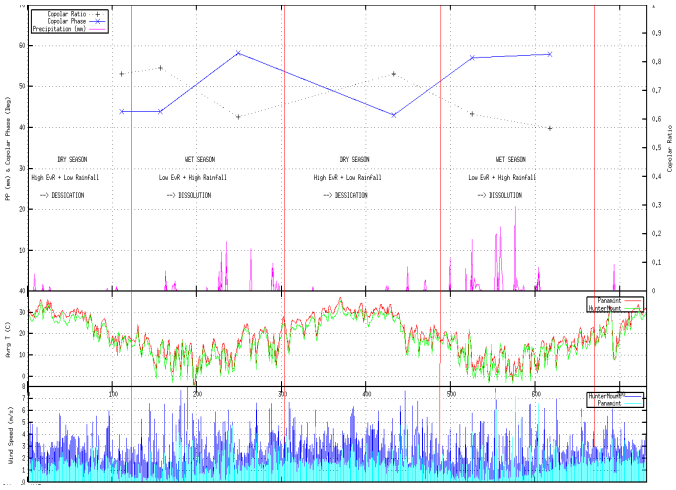

Fig. 4. Correlation between the copolar parameters extracted from the temporal ALOS/PALSAR series and the weather data provided by the USGS.

TABLE I
MEAN VALUE OF THE COPOLARIZED PARAMETERS EXTRACTED FROM SIR-C AND AIRSAR IMAGES FOR C- AND L-BANDS.

SIR-C	σ_{hh}/σ_{vv}	ϕ_{HHVV}	Frequency	Date of Flight
PR11318	0.23	11.5°	C-Band	04/16/1994
PR17826	0.23	10.4°	C-Band	04/16/1994
PR44393	0.48	6.8°	C-Band	09/30/1994
PR50316	0.49	7.6°	C-Band	09/30/1994
PR11317	0.33	24.2°	L-Band	04/16/1994
PR17825	0.32	23.4°	L-Band	04/16/1994
PR44392	0.43	10.1°	L-Band	09/30/1994
PR50315	0.42	10.8°	L-Band	09/30/1994
AIRSAR	σ_{hh}/σ_{vv}	ϕ_{HHVV}	Frequency	Date of Flight
cm6507	0.13	14.6°	C-Band	04/10/1994
cm6838	0.13	16.3°	C-Band	04/10/1994
cm6507	0.25	33°	L-Band	04/10/1994
cm6838	0.23	35.1°	L-Band	04/10/1994

for the copolar ratio.

From Table I and Fig. 4, a strong correlation between the radar phase signal and the copolar ratio can be observed as well as a strong dependency on the seasonal data. For each frequency, ϕ_{HHVV} appears to vary inversely to σ_{hh}/σ_{vv}. As an example, for the SIR-C L-band data, ϕ_{HHVV} decreases from 24° to 10.5° for an increment in σ_{hh}/σ_{vv} from 0.32 to 0.43. The same observation can be done for C-band. Variations in ϕ_{HHVV} is also related to the weather and climatic conditions as shown on Fig. 4. Such a variation supports the assumption of [27] and [28], that is the copolar phase signal is related to the moisture content of soils: the highest the soil water content, the highest the radar phase difference.

IV. COMPARISON TO ANALYTICAL IEM SIMULATIONS

In this section, we compare the values generated by a 2-layer IEM scattering model with those derived from SIR-C and AIRSAR images in order to better understand the influence of salinity in SAR imagery. The comparison is split up into April and September cases. Moreover, depending on the season, we considered both roughness parameters and complex permittivities related to each layer according to measurements performed in situ and in laboratory. All the measured and computed copolar ratios and phases are reported in Table II.

Considering the wet case, it can be seen that the IEM simulations predict copolar ratio in good agreement with values derived from L- and C-band SIR-C data. As far as the AIRSAR simulations are concerned, if we observed good agreement for C-band, some discrepancies occur when considering the L-band frequency, with an underestimated copolar ratio. According to the IEM simulations, such a ratio suggests higher soil moisture content leading to higher dielectric properties than the one expected, since $\sigma^o_{hh}/\sigma^o_{vv}$ was shown to decrease with increment in complex permittivity.

If the IEM simulations provide good agreement for the values extracted from SAR data for the wet period, they tend to overestimate $\sigma^o_{hh}/\sigma^o_{vv}$ for the dry period. Assuming the L, and C-band dielectric properties of the dry NaCl layer measured over the saltpan as representative of the ones occurring during the dry period, the 2-layer IEM simulations, with respect to SIR-C parameters, predict a higher $\sigma^o_{hh}/\sigma^o_{vv}$. Such a discrepency could be explained by the multiple scattering term we didn't consider, and that should lead to a decrease in $\sigma^o_{hh}/\sigma^o_{vv}$, since such a term has shown to differentiate the hh and vv backscattering coefficients [28].

Compared to the L- and C-bands SIR-C data, the IEM simulations of the copolar phase difference allow to correlate the variations of ϕ_{HHVV} to the seasonal variations of the dielectric properties due to changes in soil moisture between April and September. The theoretical dynamic of ϕ_{HHVV} between April and September presents the same behavior as the one observed on the SIR-C images although the simulated copolar phase predicts an higher increase than the one observed on SIR-C images. This difference can be explained by the

TABLE II
COMPARISON BETWEEN THE COPOLARIZED RATIOS σ_{hh}/σ_{vv} AND PHASE DIFFERENCES ϕ_{HHVV} EXTRACTED FROM SIR-C/X-SAR AND AIRSAR IMAGES AND THE ONES DERIVED FROM IEM SIMULATIONS AT BOTH C- AND L-BANDS.

April Season	σ_{hh}/σ_{vv} (C-band)	ϕ_{HHVV} (C-band)	σ_{hh}/σ_{vv} (L-band)	ϕ_{HHVV} (L-band)
SIR-C SAR Data	0.23	10.4°-11.5°	0.32-0.33	23.4°-24.2°
SIR-C (IEM)	0.23	9°	0.29	26°
AIRSAR SAR Data	0.13	14.6°-16.3°	0.23-0.25	33°-35.1°
AIRSAR (IEM)	0.15	15°	0.2 - 0.21	32°
September Season	σ_{hh}/σ_{vv} (C-band)	ϕ_{HHVV} (C-band)	σ_{hh}/σ_{vv} (L-band)	ϕ_{HHVV} (L-band)
SIR-C SAR Data	0.48-0.49	6.8°-7.6°	0.42-0.43	10.1°-10.8°
SIR-C (IEM)	0.64-0.68	$< 4°$	0.50-0.54	$< 6°$

underestimation of the copolar phase difference in September, since the multiple scattering term hasn't been considered. As demonstrated in [28], multiple scattering will contribute to depolarize the incident wave, leading to an additional phase difference term. According to the roughness parameter dimensions, multiple scattering have then to be taken into account, especially for C-band simulations, and should result in an increase of the copolar phase signal.

V. SUMMARY AND CONCLUSION

Based on temporal airborne and spaceborne SAR series acquired over the saltpan of Death Valley (CA), as well as on electromagnetic characterization and analytical IEM simulations, we highlighted the abilities of SAR system to follow the dynamics of hyper-saline deposits, through the variation in their soil moisture contents. Moreover, assuming complex dielectric constants derived from laboratory and f eldwork measurements as input parameters for the IEM scattering model, analytical simulations allowed to reproduce the seasonal variations of both the copolar backscattering ratio and phase difference observed on SAR images, and correlated to the saline deposits. Providing a fairly good estimation of $\sigma^o_{hh}/\sigma^o_{vv}$ and ϕ_{HHVV} derived from SAR data, the IEM simulations also allowed relating these specif c copolarized signals to the seasonal variations of the complex permittivity of soils, and conf rmed the dependency of the copolar ratio and phase difference on both the moisture and salinity of the soils.

ACKNOWLEDGMENT

The authors would like to thank Oak Ridge Associated Universities (ORAU) NASA Postdoctoral Programs which granted this research carried out at the JPL/CalTech under a contract with the National Aeronautics and Space Administration.

REFERENCES

[1] Y. Lasne, Ph. Paillou, A. Freeman, T. Farr, K. McDonald, G. Ruff é, J.-M. Malézieux, and B. Chapman, "Study of Hyper-Saline Deposits and Analysis of their Signature in Airborne and Spaceborne SAR Data: Example of Death Valley, California," *IEEE TGRS*, in press, 2009.

[2] Z. Aly, F. J. Bonn, and R. Magagi, "Analysis of the backscattering coeff cient of salt-affected soils using modeling and RADARSAT-1 SAR data," *IEEE TGRS*, vol. 45, pp. 332-341, 2007.

[3] Y. Shao, Q. Hu, H. Guo, Y. Lu, Q. Dong, and C. Han, "Effect of dielectric properties of moist salinized soils on backscattering coeff cients extracted from RADARSAT image," *IEEE TGRS*, vol. 41, pp. 1879-1888, 2003.

[4] G. Wadge, and D. J. Archer, "Evaporation of groundwater from arid playas measured by C-band SAR," *IEEE TGRS*, vol. 41, pp. 1641-1650, 2003.

[5] Y. Lasne, Ph. Paillou, A. Freeman, T. Farr, K. McDonald, G. Ruff é, J.-M. Malézieux, B. Chapman, and F. Demontoux, "Effect of salinity on the dielectric properties of geological materials: Implication for soil moisture detection by means of radar remote sensing," *IEEE TGRS*, vol. 46, pp. 1674-1688, 2008.

[6] J. B. Hasted, D. M. Ritson, and C. H. Collie, "Dielectric properties of aqueous ionic solutions. Parts I and II," *J. Chem. Phys.*, vol. 16, pp. 1-21, 1948.

[7] H. Falkenhagen, "The principal ideas in the interionic attraction theory of strong electrolytes," *Reviews of Modern Physics*, vol. 3, pp. 412-426, 1931.

[8] A. Stogryn, "Equations for calculating the dielectric constant of saline water," *IEEE TMTT*, pp.733-736, 1971.

[9] J. R. Wang, and T. J. Schmugge, "An empirical model for the complex dielectric permittivity of soils as a function of water content", *IEEE TGRS*, vol. **GE-18**, pp. 288-295, 1980.

[10] M. C. Dobson, F. T. Ulaby, M. T. Hallikainen, and M. A. El-Rayes, "Microwave dielectric behavior of wet soil - Part II: Dielectric mixing models", *IEEE TGRS*, vol. **GE-23**, pp. 35-46, 1985.

[11] K. Sreenivas, L. Venkataraknam, and P. V. Narasimha Rao, "Dielectric properties of salt-affected soils," *Int. J. Remote Sens.*, vol. 16, pp. 641-649, 1995.

[12] Z. Aly, F. Bonn, and R. Magagi, "Modelling the backscattering coeff cient of salt-affected soils: applications to Wadi el Natrun bottom, Egypt," *EARSel Proceedings 3*, pp. 372-381, 2004.

[13] F. T. Ulaby, R. K. Moore, and A. K. Fung, *Microwave Remote Sensing: Active and Passive*, Norwood, MA: Artech House, Appendix E, pp. 2017-2119, 1981.

[14] A.K. Fung, *Microwave Scattering and Emissions Models and Their Applications*, Norwood, MA: Artech House, 1994.

[15] R. Bindlish, and A. P. Barros, "Subpixel variability on remotely sensed soil moisture: An inter-comparison study of SAR and ESTAR," *IEEE TGRS*, vol. 40, pp. 326-337, 2002.

[16] F. T. Ulaby, P. P. Batlivala, and M. C. Dobson, "Microwave backscatter dependency on surface roughness, soil moisture, and soil texture, Part I - Bare soil," *IEEE TGE*, vol. **GE-16**, pp. 286-295, 1978.

[17] P. Dubois, J. van Zyl, and T. Engman, "Measuring soil moisture with imaging radar," *IEEE TGRS*, vol. 33, pp. 915-926, 1995.

[18] N. F. Glenn and J. R. Carr, "Establishing a relationship between soil moisture and RADARSAT-1 SAR data obtained over the Great Basin Nevada, USA," *Can. J. Remote Sens.*,vol. 30, no. 2, PP. 176-181, 2004.

[19] Y. Oh, K. Sarabandi, and F. T. Uaby, ”An empirical model and an inversion technique for radar scattering from bare soil surfaces,” *IEEE TGRS*, vol. 30, no. 2, pp. 370-381, 1992.

[20] Q. Hu, Y. Shao, and H. Guo, ”Microwave dielectric behavior of moistsalt soil - Experimental observations and improve dielectric models,” *Proceedings of IGARSS 2003*.

[21] Z. M. Abdel-Razak, F. Bonn, L. P. Giugni, and A. Mahmood, ”Potentiality of RADARSAT-1 images in the detection of salt affected soils in the arid zone: Wadi El-Natrun, Egypt,” *Proceedings of IGARSS 2003*.

[22] D. Bell, C. Menges, W. Ahmad, and J.J. van Zyl, ”The application of dielectric retrieval algorithms for mapping soil salinity in a tropical coastal environment using polarimetric airborne SAR,” *RSE*, vol. 75, pp. 375-384, 2001.

[23] C. B. Hunt, T. W. Robinson, W. A. Bowles, and A. L. Washburn, ”General geology of Death Valley, California - Hydrologic basin, Death Valley, California: a description of the hydrology, geochemistry, and patterned ground of the saltpan,” *USGS Prof. Paper 494-B*, Washington D. C., 138p., 1966.

[24] M. A. Kohler, T. J. Nordenson, and W. E. Fox, ”Evaporation from pans and lakes,” *U. S. Weather Bureau Research Paper 38*, 21 p., 1955.

[25] J. Shi, J. Wang, A. Y. Hsu, P. E. O’Neill, and E. T. Engman, ”Estimation of bare surface soil moisture and surface roughness parameter using L-Band SAR image data,” *IEEE TGRS*, vol. 35, pp. 1254-1266, 1997.

[26] J. J. van Zyl, and Y. Kim, ”A quantitative comparison of soil moisture inversion algorithm,” *Proceedings of IGARSS’01*, vol. **1**, pp. 37-39, 2001.

[27] Y. Lasne, Ph. Paillou, Th. August-Bernex, G. Ruff é, and G. Grandjean, ”A phase signature for detecting wet subsurface structures using polarimetric L-band SAR,” *IEEE TGRS*, vol. 42, pp. 1683-1694, 2004.

[28] Y. Lasne, Ph. Paillou, G. Ruff é, and M. Crapeau, ”Effect of multiple scattering on the phase signature of wet subsurface structures: Applications to polarimetric L- and C-band SAR,” *IEEE TGRS*, vol. **43**, pp. 1716-1726, 2005.